

# Synthesis and thermal studies of the cobalt zinc ferrous fumarato-hydrazinate

## A precursor to obtain nanosize ferrites

L. R. Gonsalves · V. M. S. Verenkar

CTAS2011 Conference Special Chapter  
© Akadémiai Kiadó, Budapest, Hungary 2012

**Abstract** Nanosize  $\text{Co}_{1-x}\text{Zn}_x\text{Fe}_2\text{O}_4$  ( $x = 0, 0.1, 0.3,$  and  $0.4$ ) have been synthesized by the precursor combustion technique via autocatalytic combustion of the mixed-metal fumarato-hydrazinate precursors. A key feature of these precursors is that they decompose autocatalytically once ignited to give the monophasic nanocrystalline ferrite. This fact is confirmed by X-ray powder diffraction analysis. The thermal decomposition pattern of the precursors has been studied by thermogravimetric and differential thermal analysis. The precursors have also been characterized by FTIR and chemical analysis to fix the chemical composition. The Curie temperature ( $T_c$ ) of the “as-prepared” oxide was determined by alternating current susceptibility measurements.

**Keywords** Nanoparticles · Co–Zn ferrite · Magnetic properties · Thermal analysis · Fumarato-hydrazinate precursor

### Introduction

Over the years, magnetic materials have been widely studied for their technological relevance, but now with the evolution of novel properties associated with material dimensions they are gaining more popularity among researchers. So understandably, development of synthetic techniques to prepare nanomaterials has taken center stage. Among the various magnetic materials, the spinel ferrite is a widely studied class due to its remarkable magnetic and

electric properties having myriad of applications in high-density recording media, microwave devices, as components of electronic devices, magnetic fluids, medical diagnostics, humidity sensors, etc., [1–6]. A great number of methods have been developed and successfully employed to synthesize such materials. Some of these include spray pyrolysis method, microemulsion synthesis, hydrothermal synthesis, reverse micelle technique, etc., [7–13].

The present study reports the synthesis of cobalt zinc ferrite nanoparticles by employing the precursor combustion technique devised 16 years back [14–19]. This technique makes use of novel precursors which are hydrazine derivatives of metal carboxylates. These metal hydrazine carboxylates being pyrophoric in nature, decompose at low temperatures leading to ultrafine oxide having high surface area. Hydrazine being a fuel aids in the combustion process by lowering the decomposition temperature of the metal complexes [20]. The thermal reactivity of the metal-hydrazine complexes is also noteworthy as the stability of the complexes changes dramatically depending on the anion and cation [21]. This report demonstrates the thermal decomposition pattern of the cobalt zinc ferrous fumarato-hydrazinate precursors which yields nanosized  $\text{Co}_{1-x}\text{Zn}_x\text{Fe}_2\text{O}_4$  ( $x = 0, 0.1, 0.3,$  and  $0.4$ ) as the only product of decomposition.

### Experimental

#### Preparation of cobalt zinc ferrous fumarato-hydrazinate

The cobalt zinc ferrous fumarato-hydrazinate precursors were synthesized by employing the method reported earlier [22]. A requisite quantity of sodium fumarate in aqueous medium was stirred with hydrazine hydrate,  $\text{N}_2\text{H}_4\cdot\text{H}_2\text{O}$

L. R. Gonsalves · V. M. S. Verenkar (✉)  
Department of Chemistry, Goa University, Taleigao Plateau,  
Goa 403 206, India  
e-mail: vmsv@rediffmail.com

(99–100%) in an inert nitrogen atmosphere for 2 h. To this, a freshly prepared solution containing ferrous chloride mixed with zinc chloride and cobalt chloride in stoichiometric amount was added dropwise with constant stirring. The precipitate thus obtained was filtered, washed with ethanol, dried with diethyl ether, and stored in a vacuum desiccator.

#### Methods of characterization

The precursors were chemically analyzed by titrimetry to determine the hydrazine content by using  $\text{KIO}_3$  as the titrant [23]. The percentage of cobalt, zinc, and iron was also estimated by standard methods given in the Vogel's textbook [23]. Infrared analysis of the precursors and their thermal products, i.e.,  $\text{Co}_{1-x}\text{Zn}_x\text{Fe}_2\text{O}_4$  were done on Shimadzu FTIR Prestige-21 spectrophotometer.

The thermal decomposition pattern of the precursors was studied by simultaneous differential thermal analysis (DTA) and thermogravimetric (TG) analysis on a NET-ZSCH, STA 409 PC (Luxx) analyzer, from RT to 900 °C

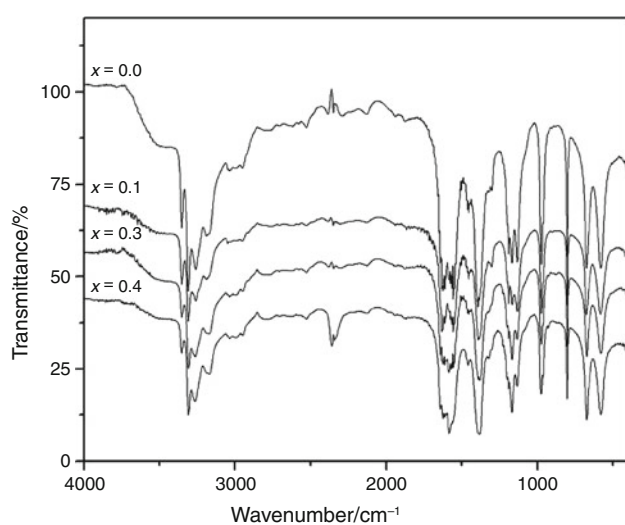


**Fig. 1** Infrared spectra of the precursor  $\text{Co}_{1-x}\text{Zn}_x(\text{C}_4\text{H}_2\text{O}_4)_3 \cdot 6\text{N}_2\text{H}_4$  ( $x = 0, 0.1, 0.3, \text{ and } 0.4$ )

in dry air. The heating rate was maintained at  $10 \text{ }^\circ\text{C min}^{-1}$ . The total weight loss studies of the samples were also carried out at a predetermined temperature. The Curie temperature was measured from the variation of alternating current susceptibility as a function of temperatures as described elsewhere [20].

#### Autocatalytic decomposition of the precursor

The dried precursors were spread on a Petri dish and ignited with a burning splinter. A small portion of it caught fire which spreads immediately to the entire bulk. The precursors decompose autocatalytically in this manner, in an ordinary atmosphere, to yield nanosize particles of the ferrite.

## Results and discussion

#### Chemical formula determination of cobalt nickel ferrous fumarato-hydrazinate

The infrared spectra of all the complexes (Fig. 1) show three absorption bands in the regions in the range  $3,180\text{--}3,355 \text{ cm}^{-1}$  due to the N–H stretching frequencies. The N–N stretching frequencies at  $\sim 974 \text{ cm}^{-1}$  prove the bidentate bridging nature of the hydrazine ligand [24]. The asymmetric and symmetric stretching frequencies of the carboxylate ions are seen at  $\sim 1,580$  and  $\sim 1,383 \text{ cm}^{-1}$ , respectively, with the  $\Delta\nu$  ( $\nu_{\text{asy}} - \nu_{\text{sym}}$ ) separation of  $202 \text{ cm}^{-1}$ , which indicate the monodentate linkage of both carboxylate groups in the dianion. The IR data confirms the formation of cobalt nickel ferrous fumarato-hydrazinate in all of the complexes.

The chemical formula,  $\text{Co}_{1-x}\text{Zn}_x\text{Fe}_2(\text{C}_4\text{H}_2\text{O}_4)_3 \cdot 6\text{N}_2\text{H}_4$  has been assigned to the complex, cobalt zinc ferrous fumarato-hydrazinate based on the observed percentage of hydrazine, cobalt, zinc, and iron which matches closely with the calculated values (Table 1). Similarly, the observed mass loss in the total mass loss studies ( $\sim 800 \text{ }^\circ\text{C}$ ) matches with the calculated value based on the above mentioned formula.

**Table 1** Chemical analysis and total weight loss data of cobalt zinc ferrous fumarato-hydrazinate precursor,  $\text{Co}_{1-x}\text{Zn}_x\text{Fe}_2(\text{C}_4\text{H}_2\text{O}_4)_3 \cdot 6\text{N}_2\text{H}_4$  ( $x = 0, 0.1, 0.3, \text{ and } 0.4$ )

Complex	Cobalt/%		Zinc/%		Iron/%		Hydrazine/%		Weight loss/%	
	Obs.	Cal.	Obs.	Cal.	Obs.	Cal.	Obs.	Cal.	Obs.	Cal.
$\text{CoFe}_2(\text{C}_4\text{H}_2\text{O}_4)_3 \cdot 6\text{N}_2\text{H}_4$	8.29	8.36	–	–	15.82	15.85	27.29	27.25	66.66	66.70
$\text{Co}_{0.9}\text{Zn}_{0.1}\text{Fe}_2(\text{C}_4\text{H}_2\text{O}_4)_3 \cdot 6\text{N}_2\text{H}_4$	7.45	7.52	0.89	0.9	15.83	15.84	27.10	27.22	66.58	66.64
$\text{Co}_{0.7}\text{Zn}_{0.3}\text{Fe}_2(\text{C}_4\text{H}_2\text{O}_4)_3 \cdot 6\text{N}_2\text{H}_4$	5.80	5.84	2.73	2.8	15.77	15.81	26.60	27.17	66.43	66.52
$\text{Co}_{0.6}\text{Zn}_{0.4}\text{Fe}_2(\text{C}_4\text{H}_2\text{O}_4)_3 \cdot 6\text{N}_2\text{H}_4$	4.99	5.00	3.66	3.7	15.75	15.79	26.43	27.15	66.39	66.46

## Thermal analysis of the precursor

The TG-DTA thermal decomposition patterns of  $\text{Co}_{1-x}\text{Zn}_x\text{Fe}_2(\text{C}_4\text{H}_2\text{O}_4)_3 \cdot 6\text{N}_2\text{H}_4$  ( $x = 0.0, 0.1, 0.3, \text{ and } 0.4$ ) are shown in Fig. 2. The TG curve of all the complexes, from room temperature (RT) to 900 °C shows three mass loss regions with two major ones. The precursor with  $x = 0$  shows a mass loss of 8.95 and 17.58% from RT to 100 °C and from 100 °C to 210 °C due to the loss of two and four  $\text{N}_2\text{H}_4$  molecules, respectively. The DTA curve shows a small exothermic hump followed by a sharp exothermic peak at 191.7 °C due to dehydrazination, as explained. The major mass loss of 35.45% from 210 °C to 320 °C was due to decarboxylation of the dehydrazinated precursor. DTA curve shows one sharp peak in this region at 318 °C due to oxidative decarboxylation. A marginal mass loss of 4.32% was observed from 320 °C to 900 °C due to oxidation of unburned carbon. However, the precursor having the composition  $x = 0.3$ , although decomposes in a similar way, it loses four  $\text{N}_2\text{H}_4$  molecule first at 154.8 °C followed by loss of two  $\text{N}_2\text{H}_4$  molecules at 189 °C as seen in the DTA curve while the TG shows mass losses of 20.26%

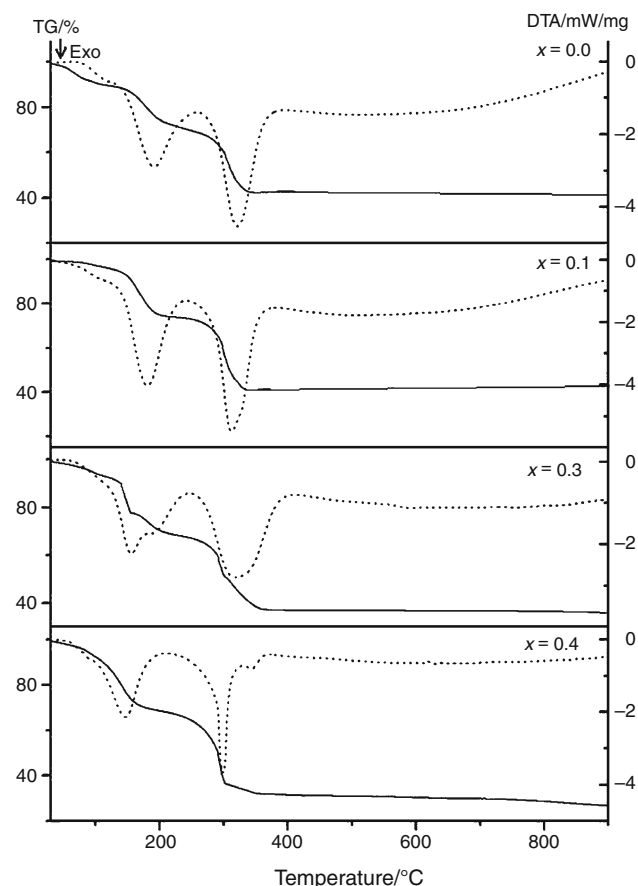


**Fig. 2** TG-DSC curve of  $\text{Co}_{1-x}\text{Zn}_x\text{Fe}_2(\text{C}_4\text{H}_2\text{O}_4)_3 \cdot 6\text{N}_2\text{H}_4$  ( $x = 0, 0.1, 0.3, \text{ and } 0.4$ )

from RT to 160 °C and 7.58% from 160 °C to 200 °C due to dehydrazination. The major mass loss due to decarboxylation was found to be 36.28% from 200 °C to 360 °C and a corresponding exothermic peak at 312.5 °C is seen in the DTA curve. A marginal mass loss of 1.72% is also observed in the TG curve from 320 °C to 900 °C due to the combustion of unburned carbon.

The precursor with composition  $x = 0.1$  and  $x = 0.4$  decomposes in an identical manner, i.e., dehydrazination followed by decarboxylation. For  $x = 0.1$ , the TG shows a mass loss of 26.52% from RT to 210 °C due to loss of six  $\text{N}_2\text{H}_4$  molecules. Corresponding DTA peak is observed at 181.4 °C. The peak due to decarboxylation is observed at 312.5 °C and the TG shows a mass loss of 33.63% from 210 °C to 320 °C. For  $x = 0.4$ , the TG shows a mass loss of 26.58% from RT to 175 °C due to loss of six  $\text{N}_2\text{H}_4$  molecules. Corresponding DTA peak is observed at 151.9 °C. A sharp peak in DTA is observed at 310.7 °C followed by a small hump due to decarboxylation. The TG, on the other hand shows a two-step mass loss of 33.96% for the same event, from 175 °C to 340 °C. A marginal mass loss of 4.12% is observed due to the oxidation of unburned carbon from 340 °C to 900 °C.

The formation of ultrafine monophasic  $\text{Co}_{1-x}\text{Zn}_x\text{Fe}_2\text{O}_4$  nanoparticles soon after the autocatalytic thermal decomposition of the precursor has been confirmed by XRD (Fig. 3). The IR spectra (Fig. 4) of the “as-prepared” ferrites show high frequency  $\nu_1$  and low frequency  $\nu_2$  bands at around  $\sim 586$  and  $\sim 403$   $\text{cm}^{-1}$ , respectively. The  $\nu_1$  and  $\nu_2$  bands are assigned to the intrinsic vibration of the tetrahedral and octahedral groups. The Curie temperature,  $T_c$ , of the “as-prepared” ferrites was determined using alternating current susceptibility measurements (Fig. 5). The Curie temperature was found to decrease with the increase in zinc

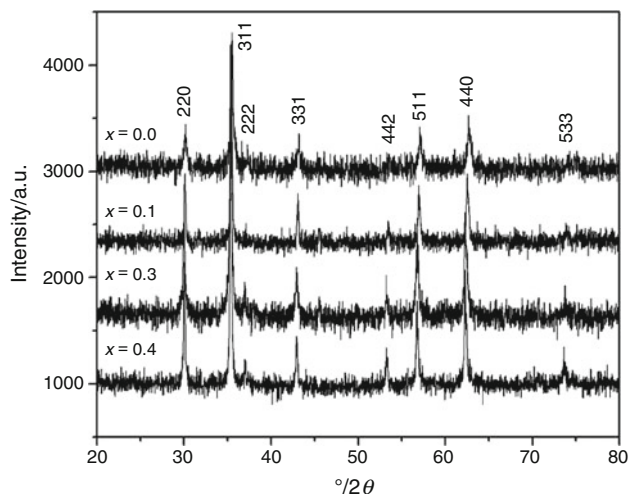


**Fig. 3** XRD pattern of “as-prepared”  $\text{Co}_{1-x}\text{Zn}_x\text{Fe}_2\text{O}_4$  ( $x = 0, 0.1, 0.3, \text{ and } 0.4$ )

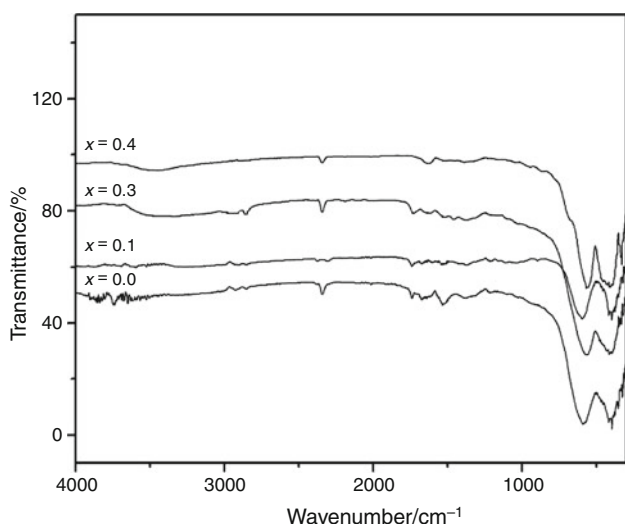


**Fig. 4** Infrared spectra of “as-prepared”  $\text{Co}_{1-x}\text{Zn}_x\text{Fe}_2\text{O}_4$  ( $x = 0, 0.1, 0.3,$  and  $0.4$ )

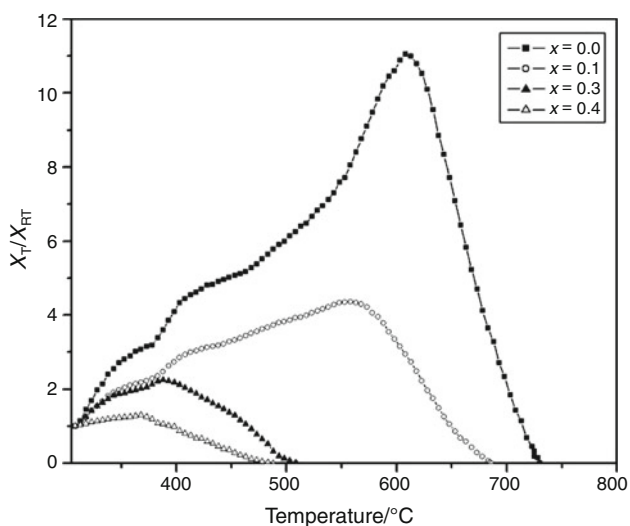


**Fig. 5** A.C. susceptibility plot of “as-prepared”  $\text{Co}_{1-x}\text{Zn}_x\text{Fe}_2\text{O}_4$  ( $x = 0, 0.1, 0.3,$  and  $0.4$ )

concentration. The  $T_c$  of cobalt ferrite,  $x = 0.0$  was found to be 730 K, whereas the samples with  $x = 0.1, 0.3,$  and  $0.4$  had a  $T_c$  of 686, 509, and 488 K, respectively. The  $T_c$  values match closely with the reported values [25].

## Conclusions

The precursor combustion technique can be successfully employed to produce uniform and ultrafine monophasic particles of mixed metal ferrite. The precursors for ultrafine ferrite by autocatalytic decomposition after its partial initial ignition. The chemical analysis, total mass loss, and

infrared spectral analysis of the precursor complexes confirms the formation and the formula  $\text{Co}_{1-x}\text{Zn}_x\text{Fe}_2(\text{C}_4\text{H}_2\text{O}_4)_3 \cdot 6\text{N}_2\text{H}_4$  ( $x = 0, 0.1, 0.3,$  and  $0.4$ ) has been fixed accordingly. The TG–DTA studies of the complexes show dehydrazination followed by a two-step decarboxylation to form  $\text{Co}_{1-x}\text{Zn}_x\text{Fe}_2\text{O}_4$ . The formation of this ultrafine single phase ferrite has been confirmed by XRD and IR. The Curie temperature of the “as-prepared” ferrites was found to be comparable with the reported values. This synthetic strategy, thus can be applied to synthesize different ferrites by suitably modifying the precursor as per the desired end product.

## References

- Ramana Reddy AV, Ranga Mohan G, Ravinder D, Boyanov BS. High-frequency dielectric behaviour of polycrystalline zinc substituted cobalt ferrites. *J Mat Sci.* 1999;34:3169–76.
- Josyulu OS, Sobhanadri J. DC conductivity and dielectric behaviour of cobalt-zinc ferrites. *Phy Stat Sol (a).* 1980;59:323–9.
- Veverka M, Veverka P, Jirak Z, Kaman O, Knizek K, Marysko M, Pollert E, Zaveta K. Synthesis and magnetic properties of  $\text{Co}_{1-x}\text{Zn}_x\text{Fe}_2\text{O}_4$  nanoparticles as materials for magnetic fluid hyperthermia. *J Magn Magn Mater.* 2010;322:2386–9.
- Matsushita N, Ichinose M, Nakagawa S, Naoe M. Co–Zn ferrite films prepared by facing targets sputtering system for longitudinal recording layer. *J Magn Magn Mater.* 1999;193:68–70.
- Mukherjee K, Majumdar SB. Hydrogen sensing characteristics of wet chemical synthesized tailored  $\text{Mg}_{0.5}\text{Zn}_{0.5}\text{Fe}_2\text{O}_4$  nanostructures. *Nanotechnology.* 2010;21:255504.
- Gedam NN, Padole PR, Rithe SK, Chaudhari GN. Ammonia gas sensor based on a spinel semiconductor,  $\text{Co}_{0.8}\text{Ni}_{0.2}\text{Fe}_2\text{O}_4$  nanomaterial. *J Sol-Gel Sci Tech.* 2009;50:296–300.
- Chen Z, Gao L. Synthesis and magnetic properties of  $\text{CoFe}_2\text{O}_4$  nanoparticles by using PEG as surfactant additive. *Mat Sci Eng B.* 2007;141:82–6.
- Vital A, Angermann A, Dittmann R, Graule T, Topfer J. Highly sinter-active (Mg–Cu)–Zn ferrite nanoparticles prepared by flame spray synthesis. *Acta Mater.* 2007;55:1955–64.
- Hua ZH, Chen RS, Li CL, Yang SG, Lu M, Gu XB, Du YW.  $\text{CoFe}_2\text{O}_4$  nanowire arrays prepared by template-electrodeposition method and further oxidation. *J Alloys Compd.* 2007;427:199–203.
- Thakur S, Katyal SC, Singh M. Structural and magnetic properties of nano nickel–zinc ferrite synthesized by reverse micelle technique. *J Magn Magn Mat.* 2009;321:1–7.
- Maensiri S, Masingboon C, Boonchom B, Seraphin S. A simple route to synthesize nickel ferrite ( $\text{NiFe}_2\text{O}_4$ ) nanoparticles using egg white. *Scripta Mater.* 2007;56(9):797–800.
- Jiang J. A facile method to the  $\text{Ni}_{0.8}\text{Co}_{0.2}\text{Fe}_2\text{O}_4$  nanocrystalline via a refluxing route in ethylene glycol. *Mater Lett.* 2007;61:3239–42.
- Singhal S, Singh J, Barthwal SK, Chandra K. Preparation and characterization of nanosize nickel-substituted cobalt ferrites ( $\text{Co}_{1-x}\text{Ni}_x\text{Fe}_2\text{O}_4$ ). *J Sol State Chem.* 2005;178:3183–9.
- Verenkar VMS, Rane KS. Thermal and electrothermal analysis (ETA) of Iron (II) carboxylato-hydrazinates Part I – Ferrous fumarato-hydrazinate and ferrous succinato-hydrazinate. In: Dharwadkar SR, Bharadwaj SR, Mukherjee SK, Sood DD,

- editors. Proceedings of the 10th national symposium on thermal analysis, thermans. Kanpur: Indian Thermal Analysis Society; 1995. p. 171–4.
- Verenkar VMS, Rane KS. Synthesis, characterization and thermal analysis of ferrous malato-hydrazinate. In: Ravindran PV, Sudersanan M, Misra NL, Venugopal V, editors. Proceedings of the 12th national symposium on thermal analysis, thermans. Gorakhpur: Indian Thermal Analysis Society; 2000. p. 194–7.
  - Sawant SY, Verenkar VMS, Mojumdar SC. Preparation, thermal, XRD, chemical and FTIR spectral analysis of  $\text{NiMn}_2\text{O}_4$  nanoparticles and respective precursor. *J Therm Anal Calorim.* 2007;90:669–72.
  - Gonsalves LR, Verenkar VMS, Mojumdar SC. Preparation and characterization of  $\text{Co}_{0.5}\text{Zn}_{0.5}\text{Fe}_2(\text{C}_4\text{H}_2\text{O}_4)_3 \cdot 6\text{N}_2\text{H}_4$  A precursor to prepare  $\text{Co}_{0.5}\text{Zn}_{0.5}\text{Fe}_2\text{O}_4$  nanoparticles. *J Therm Anal Calorim.* 2009;96(1):53–7.
  - Gonsalves LR, Verenkar VMS, Mojumdar SC. Synthesis of cobalt nickel ferrite nanoparticles via autocatalytic decomposition of the precursor. *J Therm Anal Calorim.* 2010;100:789–92.
  - Gonsalves LR, Verenkar VMS, Mojumdar SC. Synthesis and characterization of  $\text{Co}_{0.8}\text{Zn}_{0.2}\text{Fe}_2\text{O}_4$  nanoparticles. *J Therm Anal Calorim.* 2011;104:869–73.
  - More A, Verenkar VMS, Mojumdar SC. Nickel ferrite nanoparticles synthesis from novel fumarato-hydrazinate precursor. *J Therm Anal Calorim.* 2008;94(1):63–7.
  - Porob RA, Khan SZ, Mojumdar SC, Verenkar VMS. Synthesis, TG, DSC and infrared spectral study of  $\text{NiMn}_2(\text{C}_4\text{H}_4\text{O}_4)_3 \cdot 6\text{N}_2\text{H}_4$ : a precursor for  $\text{NiMn}_2\text{O}_4$  nano-particles. *J Therm Anal Calorim.* 2006;86(3):605–8.
  - Sawant SY, Kannan KR, Verenkar VMS. Synthesis, characterisation and thermal analysis of nickel manganese fumarato-hydrazinate. In: Pillai CGS, Ramakumar KL, Ravindran PV, Venugopal V, editors. Proceedings of the 13th national symposium on thermal analysis, B.A.R.C. Mumbai: Indian Thermal Analysis Society; 2002. p. 154–5.
  - Jeffery GH, Bassett J, Mendham J, Denney RC. Vogel's text book of quantitative inorganic analysis. 5th ed. England: Longman; 1989.
  - Braibanti A, Dallavalle F, Pellinghelli MA, Leporati E. The nitrogen–nitrogen stretching band in hydrazine derivatives and complexes. *Inorg Chem.* 1968;7:1430–3.
  - Gul IH, Abbasi AZ, Amin F, Anis-ur-Rehman M, Maqsood A. Structural, magnetic and electric properties of  $\text{Co}_{1-x}\text{Zn}_x\text{Fe}_2\text{O}_4$  synthesized by co-precipitation method. *J Magn Magn Mater.* 2007;311:494–9.